TD-10-003 22 February, 2010

Fabrication and Test of Corrector Dipole Package ILC_CM2_Dipole_01

N. Andreev, C. Hess, V. S. Kashikhin, F. Lewis, M. J. Kim, D. F. Orris, M. A. Tartaglia, T. Wokas

I. Requirements

In order to steer beam through the center of NML Cryomodule 2 (CM2), which is in the process of being assembled, a package containing weak horizontal and vertical corrector dipoles was specified. The original requirements specification document is included in this note as Appendix I. Note that the dipoles operate at low current, have rather low required field integral, and very loose field quality constraints. Also note that field angle and alignment tolerances have not been specified.

II. Design

The corrector package design is based on the DESY TESLA Test Facility magnet package design [1], and the original magnetic design is given in Appendix 2. The corrector cold mass dimensions were defined by the DESY LHe vessel, beam pipe, and conduction cooled current leads. As in [1] the dipole field is generated by single layer shell-type windings laid on the beam pipe outer surface. This type of design was also used for HINS solenoid correctors [2] which were successfully tested [3], [4]. The main difference between TESLA, HINS and this corrector is an outer Aluminum collar tube. This tube forms a closed mold for epoxy vacuum impregnation of the whole package, and provides coil pre-stress during cool down.

It was possible to reach the desired dipole field integral (0.01 T-m) and field uniformity (5% at radius of 5 mm) by expanding the length and increasing the radius of the HINS coil design. Figures 1 and 2 show the side and cross section views of the dipole assembly (from drawing number 5520.000-MD-461350). The outer flux return is not shown in the assembly view: it is a simple cylinder with end pieces, whose 4 inch inner diameter closely matches the outer Aluminum collar shown, and has an outer diameter of 4.88 inches. The peak magnetic field in the soft iron yoke is low enough (about .85 T at 100 A) that saturation should not be a problem. At 100 A the peak field on the coil is 0.31 T, and peak field in the bore is 0.20 Tesla (based upon the as-built dipoles, described below). The design achieves the required integral strength at about 25 A, and thus has plenty of operating margin. A 3D Opera model predicts the integrated field uniformity at the radius of 5 mm to be 0.14 %.

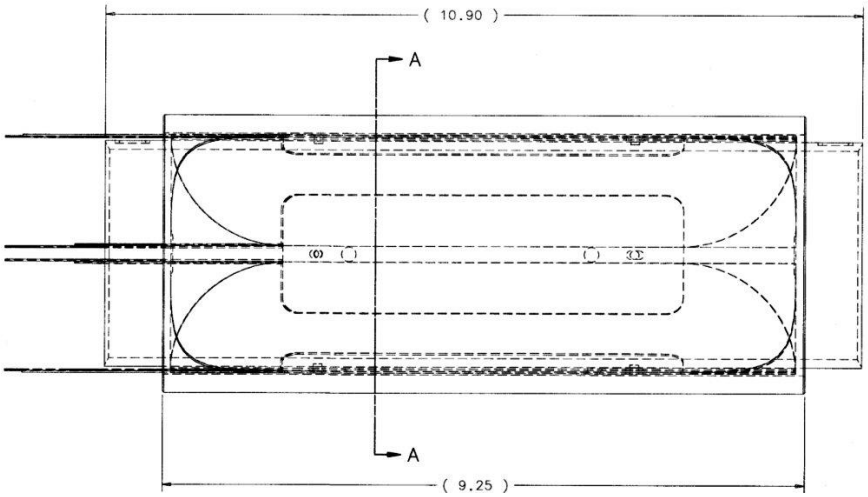

Fig. 1. Side view of dipole coil corrector coil assembly.

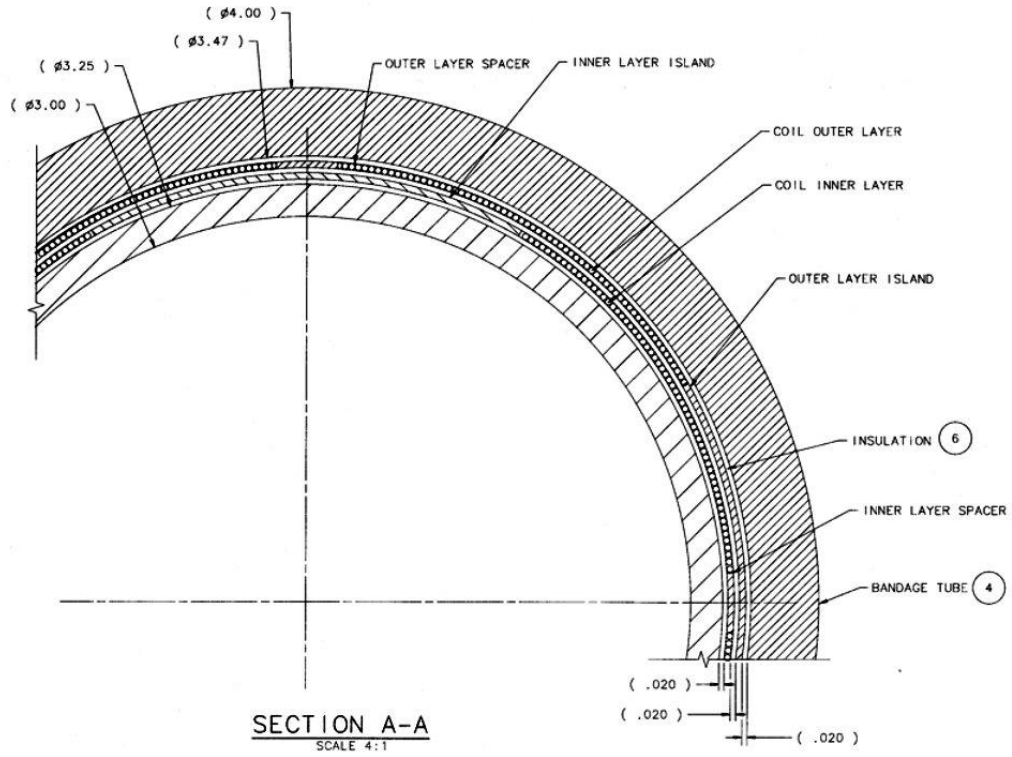

Fig. 2. Cross section of dipole assembly; outer iron flux return cylindrical shell is not shown.

III. Fabrication

The coils were wound from 0.50 mm diameter NbTi multifilament superconductor wire, with Formvar®-insulated outer diameter of 0.54 mm, having a Cu to SC ratio of 1.5±0.1:1. Table I shows the short sample performance of this wire (lot no. 412E-1, spool 1B6A) at 4.2 K, as measured by the manufacturer, Supercon, Inc. Coils for the Inner dipole, which we labeled HD (horizontal) during the test, each have 74 turns of wire. The Outer dipole coils, which we labeled VD (vertical), each have 77 turns of wire. Given the strand performance data, the expected

quench current in the dipole self-field should be above the 330 A maximum current of the power supply.

Table I. 0.50 mm Superconductor Wire Short Sample Performance at 4.2 K

Field, Tesla	9	7	5	3
Critical Current, Amperes	48	133	204	280

Features are machined into the inner mounting tube that register the coil positions, which guarantee parallel alignment for each coil and orthogonal field directions of the vertical and horizontal steering dipoles. Each coil layer is wound on a .005" B-stage tape substrate, and wrapped with ~0.015" of glass tape. A stainless steel strip (0.375" wide x .001" thick x 60" long) was spiral wound between layers for use as a quench protection heater. For quench propagation studies, two small spot heaters were attached to one of the Outer coils: one in the center and one on the end of the inner winding. Voltage taps were placed across each coil for quench protection at the "half coil" level, and to identify the quenching coil. Figure 2 shows a schematic of the coil voltage taps and spot heater placement. The completed corrector package was epoxy impregnated. A Magnet Description document that summarizes details of the device is available on the web at http://tiweb.fnal.gov/website/controller/1443. Photographs of the corrector package assembly are shown in Figures 4-7.

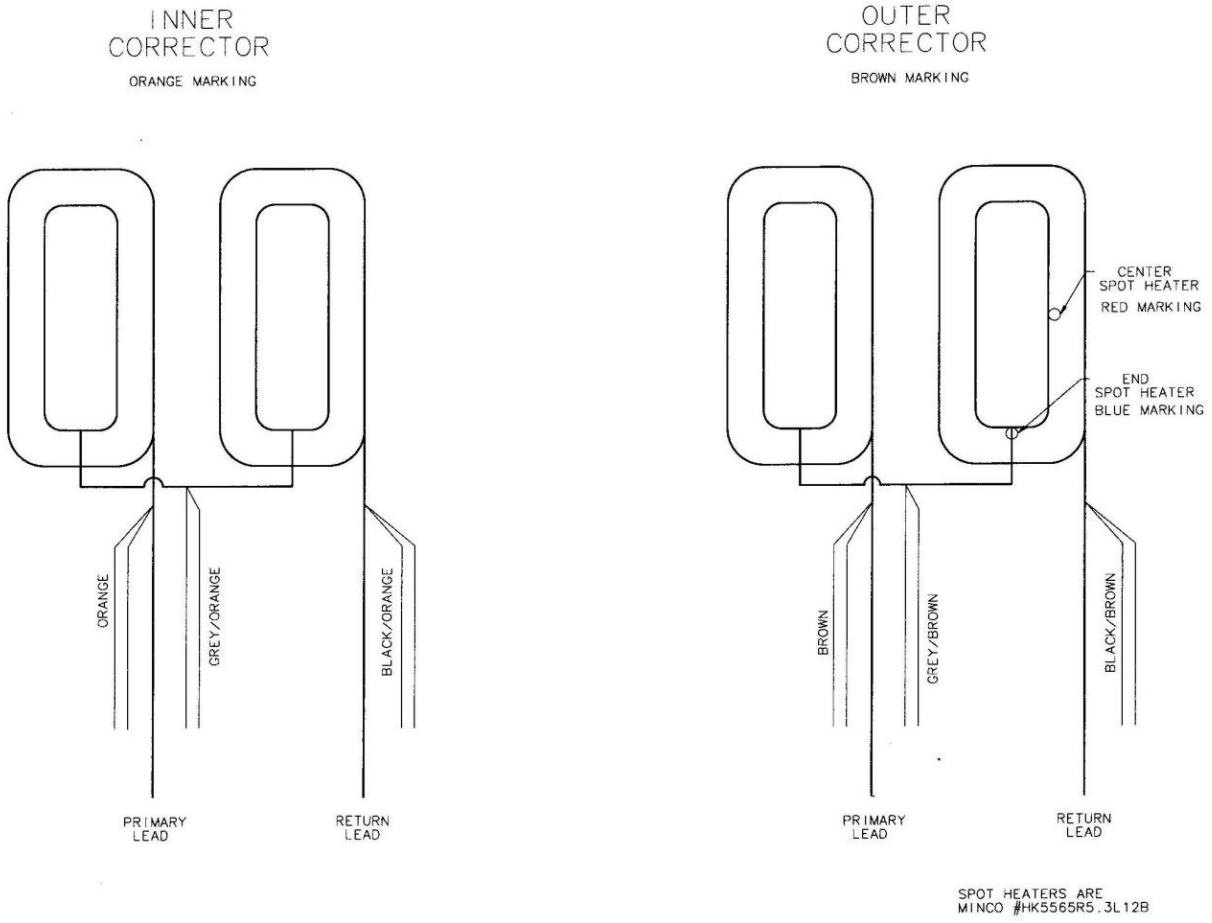

Fig. 3. Schematic of the coil voltage tap and spot heater placement.

Fig. 4. Photo of Inner dipole coil above glass cloth wrapped around inner pipe.

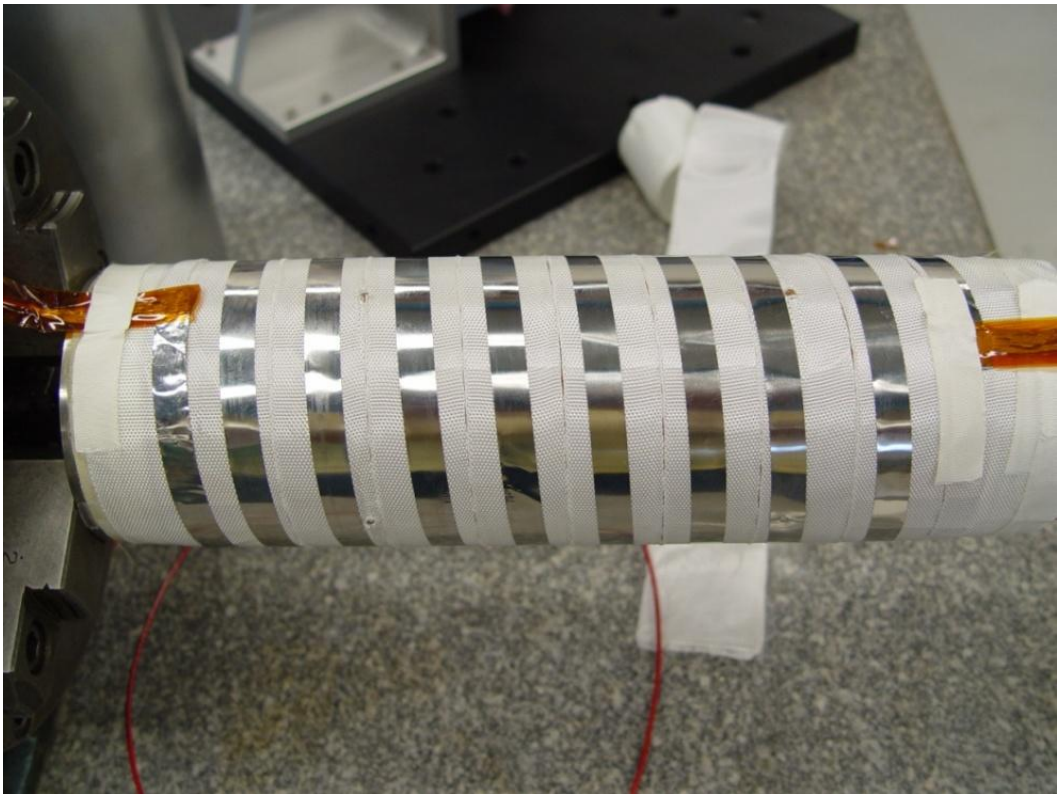

Fig. 5. Photo of strip heater wrapped in a helical spiral around Inner dipole.

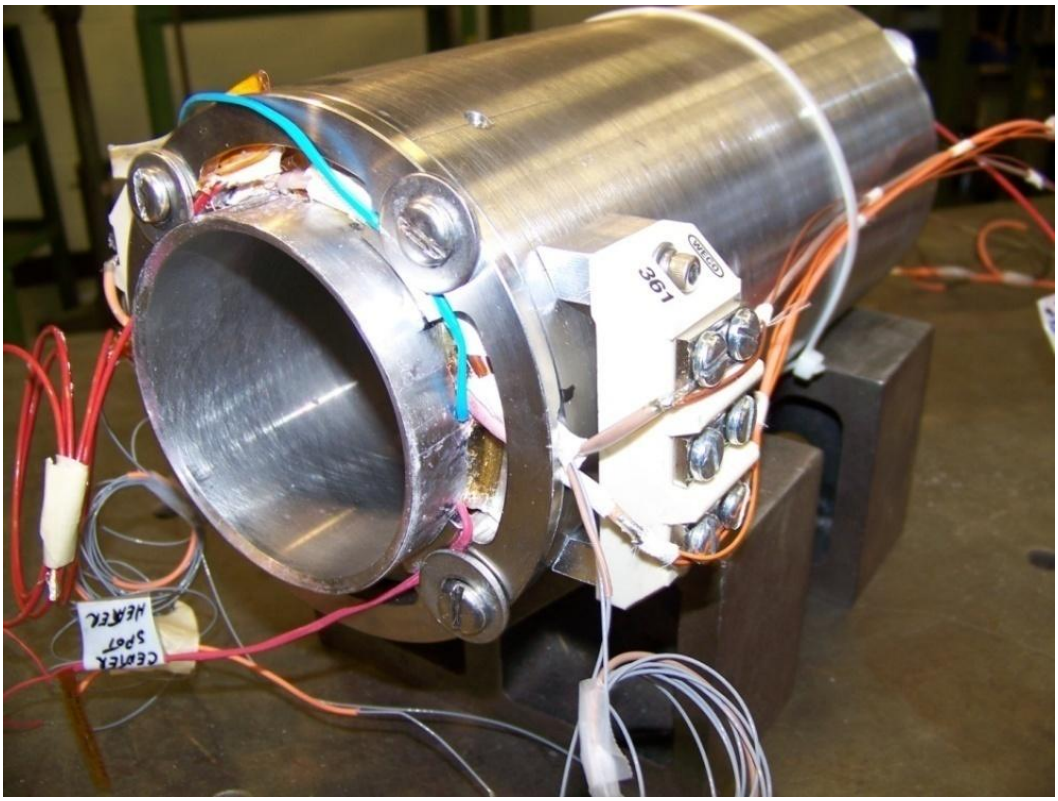

Fig. 5. Photo of the completed corrector package cold mass.

IV. Test Overview

It was not possible to study the magnet performance at 1.9 K, but a 4.4 K test in the MTF Stand 3 dewar was easily achieved by adapting to the stand 3 mechanical and instrumentation assembly. Magnetic measurements were made possible by centering the HINS warm bore tube within the corrector package inner cylinder. The mobile quench and power system MQPS-2 was used, and initially configured to power only a single coil at a time. A 1.5 Ω dump resistor for energy extraction was programmed to switch in 10 ms after quench detection, for all tests.

The corrector package was tested in three thermal cycles: on Friday 1/22/2010 the first helium cool down was performed for quench protection (strip) heater studies and magnetic measurements of the VD. The device warmed to 200 K over the weekend, followed by a second 4.4 K cool down on Monday 1/25 when VD magnetic measurements were completed up to 50 A without incurring a spontaneous quench. On 1/26 and 1/27 the strip heater studies and magnetic measurements were made on the HD, which was tested to a current of 100 A without a spontaneous quench.

Following these successful tests, it was decided to power the two dipoles in series to verify that Lorentz forces did not introduce quench performance problems. This required several days of MQPS-2 reconfiguration to protect both dipoles at once, capture additional voltage tap segments for characterization, and add another power supply for inducing spot heater quenches. The device warmed up again to 280 K during this period, and was cooled to 4.4 K a third time on 2/2/2010.

The series-powered VD+HD were ramped to 100 A without a spontaneous quench. At this time, a spot heater was fired to induce a quench: the strip heater power supply did not fire because it was not set to "protection" mode. However, the dump resistor ensured the current decayed to zero in 10 ms (which, in fact, is much faster than the heater discharge and heat diffusion time). Another ramp to 100 A without spontaneous quench demonstrated that both dipole magnets perform well to this level, and confirmed that heater protection is not necessary if a dump switch and resistor are used. (A test of self-protection, with no dump or heaters, was not attempted for this device). This quench performance test was followed with a final magnetic measurement at 100 A, and a series of spot heater-induced quenches to study quench propagation velocity as a function of the dipole current.

The device was then warmed to room temperature over several days, and was removed from the test dewar on Tuesday 2/9. The corrector package was immersed in a bath of LN_2 for several days to flush out helium, in order to reduce helium background levels during leak checking when eventually installed in a helium vessel.

V. Quench Development Studies

Two types of studies were performed during the test to understand heater effectiveness and quench propagation in the dipole coils. First, the quench protection strip heater was used to induce quenches. This study mapped out the time delay from heater firing until quench detection, as a function of heater voltage and coil current. As the strip heater is wound between the Inner and Outer coils, the same matrix of parameters was explored for both coils. For this study, the heater firing unit (HFU) was set to the minimum capacitance of 4.8 mF, to introduce the shortest possible pulse, and minimize heater current to reduce risk of damaging wire connections to the heater. With a strip heater resistance of 6 Ω at room temperature (not measured cold), the 1/e time constant is RC = 29 ms; the actual measured 1/e time constant was 22 ms. Since the heater extends over both coils, quench development was typically seen in both – although it was not very symmetric at low current – and these quenches were detected by the total dipole voltage at the 0.3 V threshold, rather than by the Half coil difference at 0.1 V threshold.

Figures 5 and 6 show the results of this study, plotted respectively as a function of the heater voltage and deposited energy. At the lowest current 10 A, the minimum HFU setting at which a quench could develop was 67 V. At 25 A and the minimum 55 V HFU setting, the quench delays (not shown in the figures) were 437 ms for VD, and 265 ms for HD. The shortest quench time delays are seen to be 20-30 ms, comparable to the strip heater-HFU time constant.

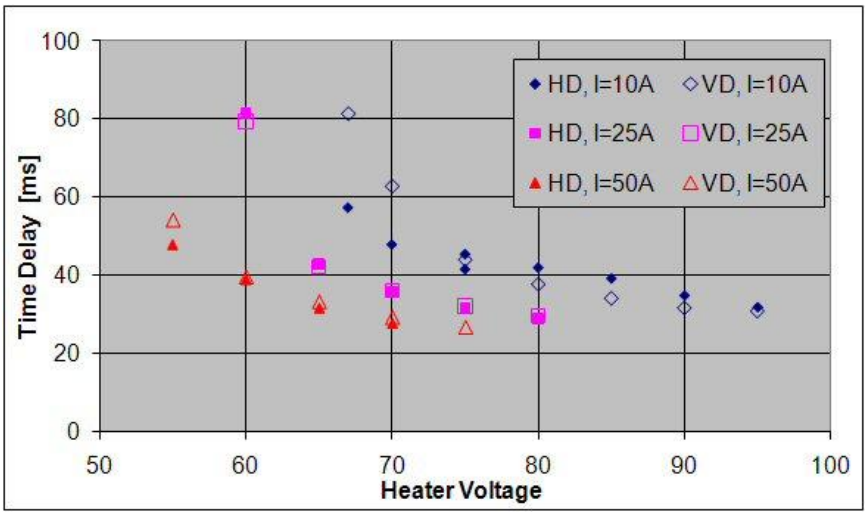

Fig. 5. Delay from heater fire to quench detection of total dipole voltage at 0.30 V, as a function of heater voltage at a range of dipole currents.

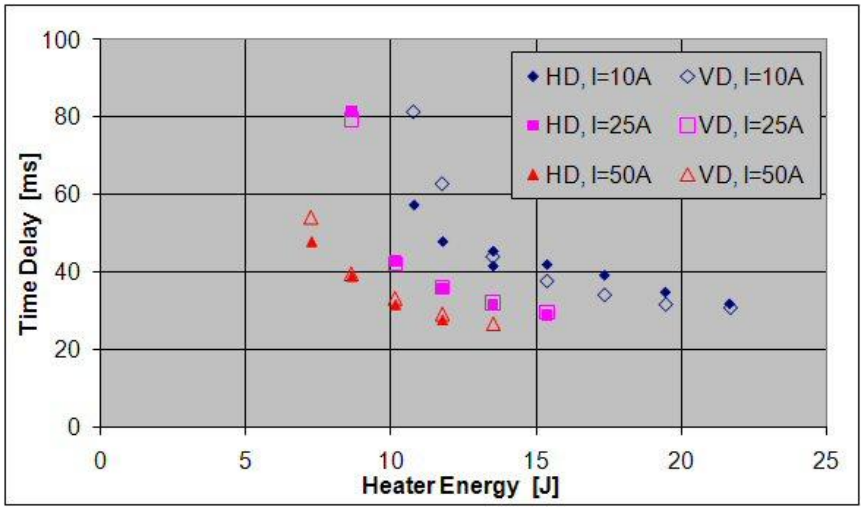

Fig. 6. Delay from heater fire to quench detection of total dipole voltage at 0.30 V, as a function of heater energy at a range of dipole currents.

The second study mapped out the quench propagation velocity for one Outer coil as a function of the dipole current, at fixed heater voltage. The spot heaters have 5.3 Ω resistance at room temperature, and subtend an area of 0.258 cm^2. For this test, the HFU was again set to the minimum capacitance, 4.8 mF, and to the minimum voltage at which it would fire, 20 V. This setting results in a local deposition of 0.96 J, of which half presumably diffuses inward to the coil. The expected RC time constant of 25 ms was consistent with the measured 27 ms 1/e time.

Quench development by either spot heater was not detected for the dipole operating at 10 A. At 20 A, the delays were very long: it took 450 ms to detect the End spot heater quench, while it was several seconds delay for the Center spot heater. The long quench development time seen here and in the low current strip heater tests implies very slow voltage development does not result in damaging the superconductor. This is very consistent with conclusions from

the HINS solenoid test program, where quench propagation in 0.6 mm and 0.8 mm superconducting lead strands was studied [5].

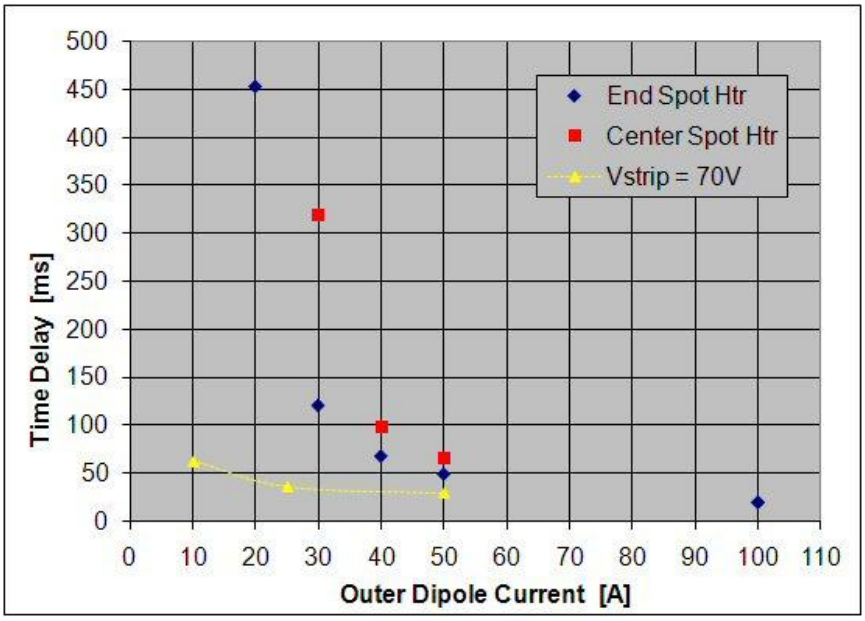

Fig. 7. Delay from spot heater fire to quench detection of half coil voltage at 0.10 V, as a function of dipole current; strip heater result at 70 V is added for comparison. Delay at 20 A for the Center spot heater was several seconds.

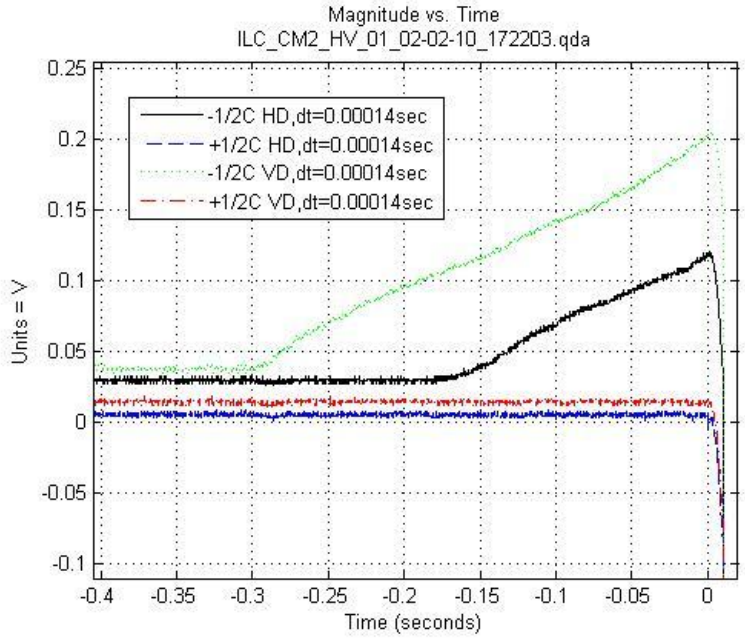

Fig. 8. Voltage development for a quench induced by the Center spot heater with both dipoles powered at 30 A. Non-zero baseline levels are due to electronic offset voltages.

Figure 8 shows a "typical" voltage development for spot-heater induced quenches; what is not so typical is that the Inner coil also quenched, with some delay. This was the case for the 20 A and 30 A Center spot heater quenches, but no others. There is more VD-HD coil overlap in the center region than on the ends (see Figs. 1 and 3), so heat may more effectively diffuse there and initiate quenching in the other dipole. From these voltage traces, we extract the time it takes for voltage to rise from zero to detection at 100 mV, and derive an average rate of voltage rise associated with quench propagation. Note in Fig. 8 that the Inner and Outer coil quenches develop with the same slope. These quench propagation velocities are plotted in Fig. 9, and are seen to be consistent with a simple 2nd order polynomial dependence on dipole current. No model has been built to predict the quench propagation in these coils or make a comparison to these data.

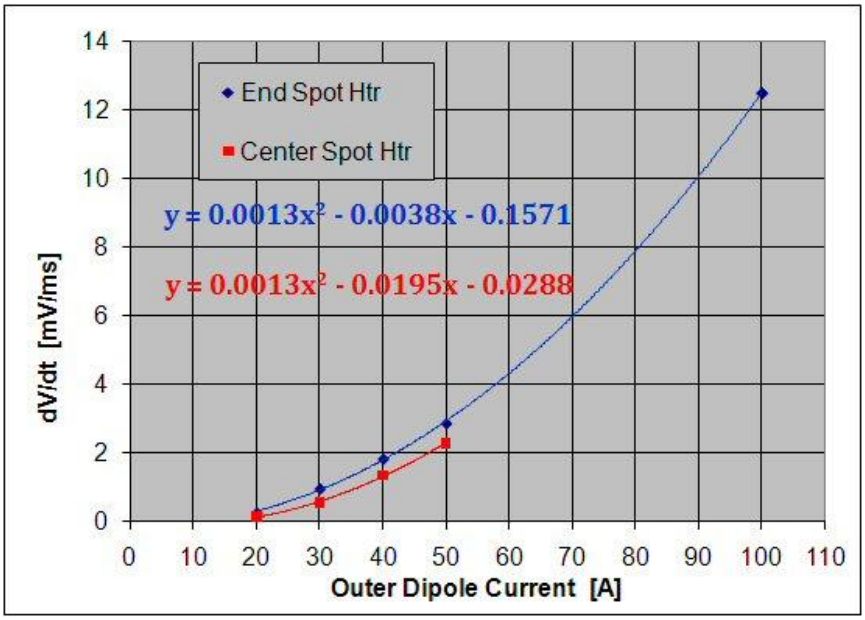

Fig. 9. Quench propagation velocity (rate of voltage rise) versus Outer Dipole current.

VI. Magnetic Measurements

Fig. 10 shows a photo of the corrector package mounted on the test stand insert, with warm bore tube and power leads clearly visible. Dipole field uniformity was not measured, although this is something that could be done at room temperature and low current in the future, if necessary, using a rotating harmonic coil probe. Two types of magnetic measurement sensors were used to map the fields from the dipoles. A 10 T range Senis 3-axis Hall probe (S/N 2605) was used to map the transverse field shapes versus position at a range of currents (to test linearity). A Bartington Mag-03MC1000 3-axis fluxgate sensor (S/N 1535) with ±10 Gauss range was used to measure the superconductor magnetization field at 0 A after ramping up and down, and to explore the fringe field at the magnet ends, up to 25 A. Hall probe X and Y axes were oriented to approximately align them with VD and HD, while the fluxgate was oriented at 45º to prevent saturation at the 10 G level.

Both probes were digitized with a Keithley 2700 multiplexing DVM (S/N 0899874). Probe vertical positions were measured by a Bausch & Lomb encoder with 10 micron resolution

(S/N 4189). The magnet current was digitized using a Danfysk transductor (FNAL No. 85314) in the PS-2 rack, which was calibrated in September 2009 to 0.1%. These devices were recorded using Labview programs on a WindowsXP® computer.

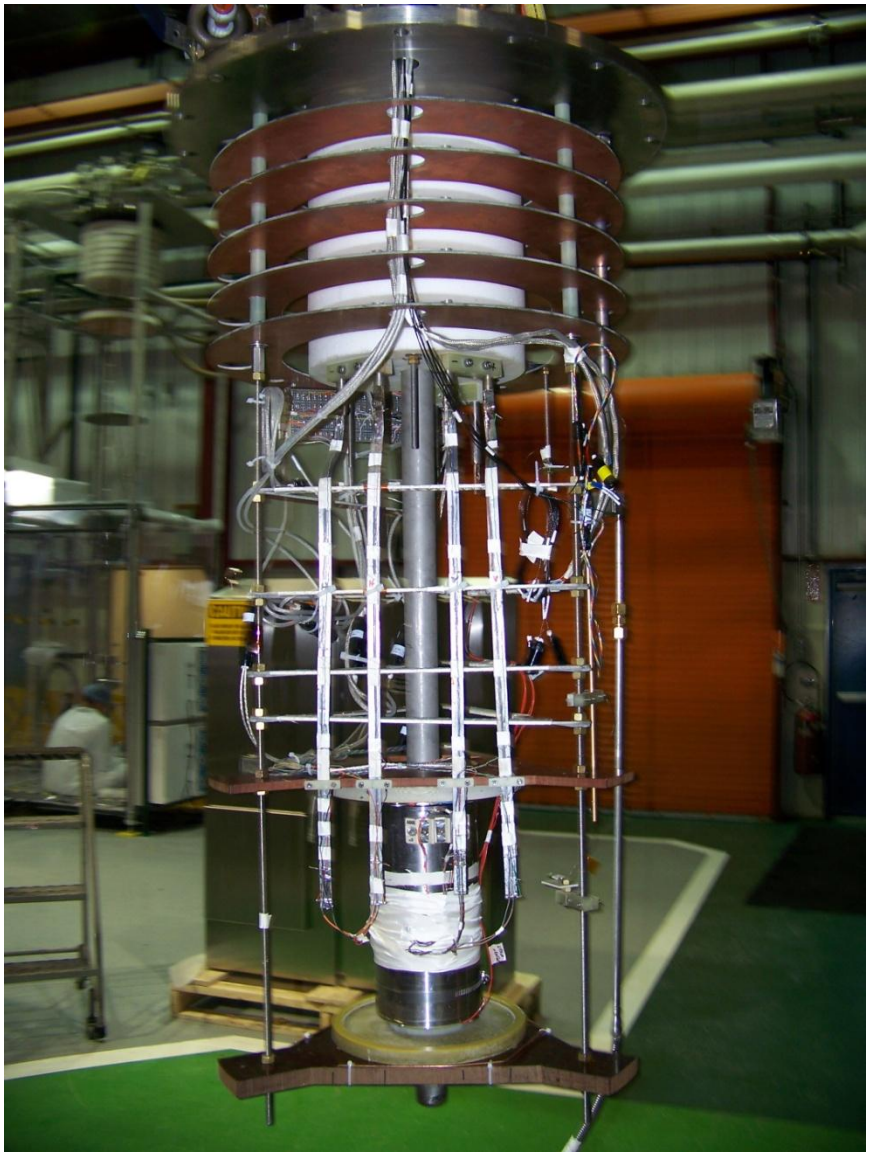

Fig. 10. Dipole corrector package mounted on stand 3 insert prior to cold test.

Figure 11 shows the comparison of the 3D as-built model with the measured transverse field profiles for both dipoles at a current of 50 A. The model slightly over-estimates the peak field (1001 vs 975 G for VD; 962 vs 944 G for HD), and slightly over-estimates the width of the distributions. For VD, the model gives 0.019 T-m at 50 A, while data integrate to 0.0181 T-m.

The same distributions are shown in Fig. 12, but on a log scale to illustrate the agreement in the fringe field region. Scatter in the low field points is comparable to stability of the absolute offset, which is on the order of several Gauss. The conclusion is that there is good agreement between data and model, and that the fringe field beyond 200 mm from the dipole center is on the level of 6 to 7 Gauss.

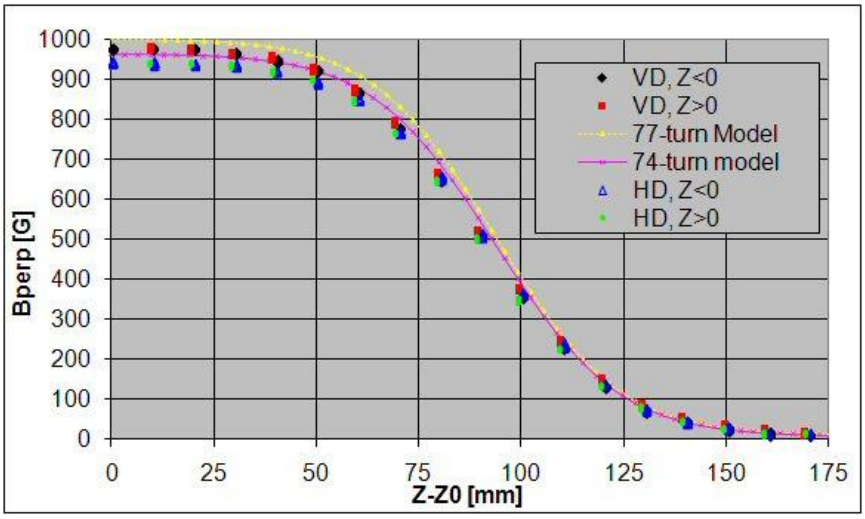

Fig. 11. Overlay of dipole transverse field profiles on axis, with 3D Opera model prediction (linear scale).

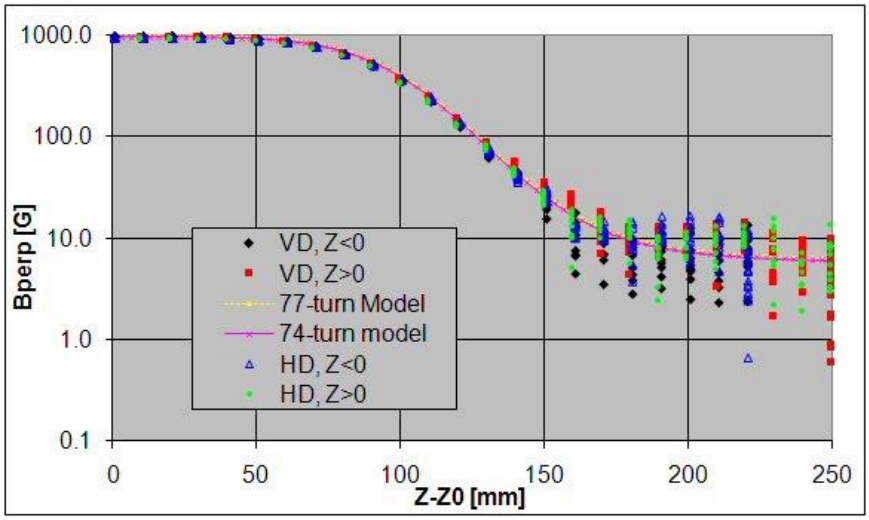

Fig. 12. Overlay of dipole transverse field profiles on axis, with 3D Opera model prediction (log scale).

The transfer function profiles for the individual dipoles at 50 A are overlaid in Fig. 13 along with the profile for the series combination. The peak transfer functions were 19.44 G/A for VD, 18.81 G/A for HD at 50 A, and 26.79 G/A in series at 100 A; this agree to 1% with the expected value, assuming orthogonal dipoles and linear behavior at these currents.

The HD central field was measured using a stair-step ramp up and down, from 50 A to 100A, then down to 0 A, in 10 A steps; the Hall probe offset was measured at the end of the ramp cycle (about -30 Gauss in each component), which therefore includes a contribution to the offset from superconductor magnetization. The result is shown in Fig. 14: the linear fit to these data give a very slight loss of strength with current, if any, and is consistent with the results presented above.

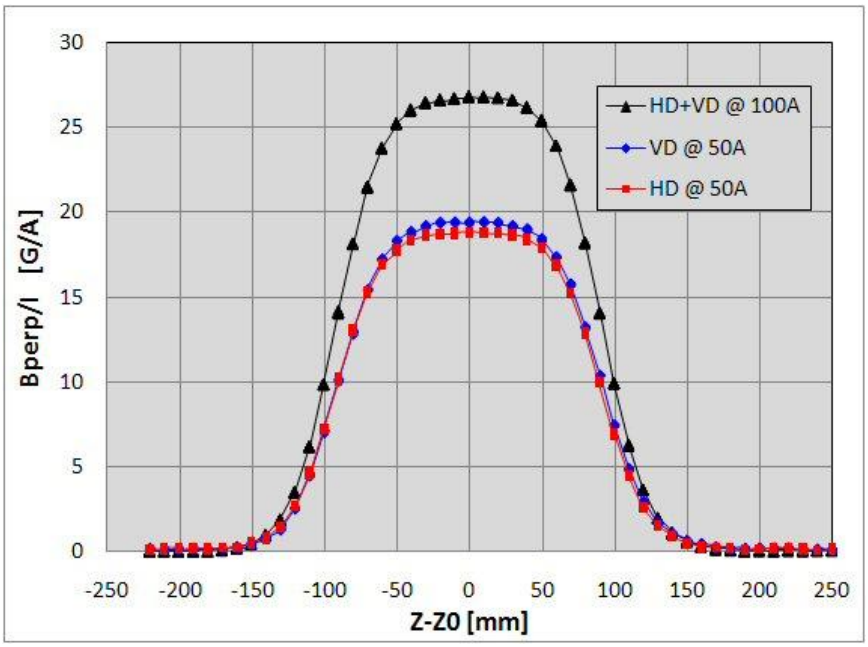

Fig. 13. Transfer function profiles of Inner and Outer dipoles at 50 A, overlaid with transverse field shape for both dipoles in series at 100 A.

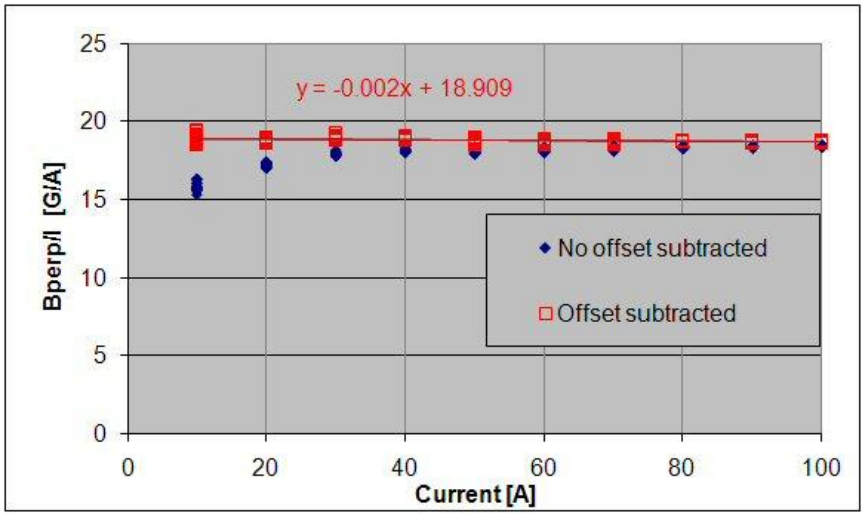

Fig. 14. Transfer Function at HD center versus current for stair-step ramp up and down.

The fluxgate sensor scans allowed precise measurement of the low fields due to superconductor and iron yoke magnetization, and in the fringe field region beyond the coil ends. The former measurement was made after the VD was ramped up to 50 A and back to zero (for the Hall probe scan). B_x and B_y probes within the fluxgate sensor are offset by 30 mm, so the scan was made in 10.0±0.01 mm steps in order to reconstruct the field magnitude by combining B_x and B_y at the same point. The resulting profile is shown in Fig. 15, which has a central field value of about 12 G. This level of the peak field implies there will be a remnant integral field of about 0.0002 T-m with the dipole off, after it has been ramped.

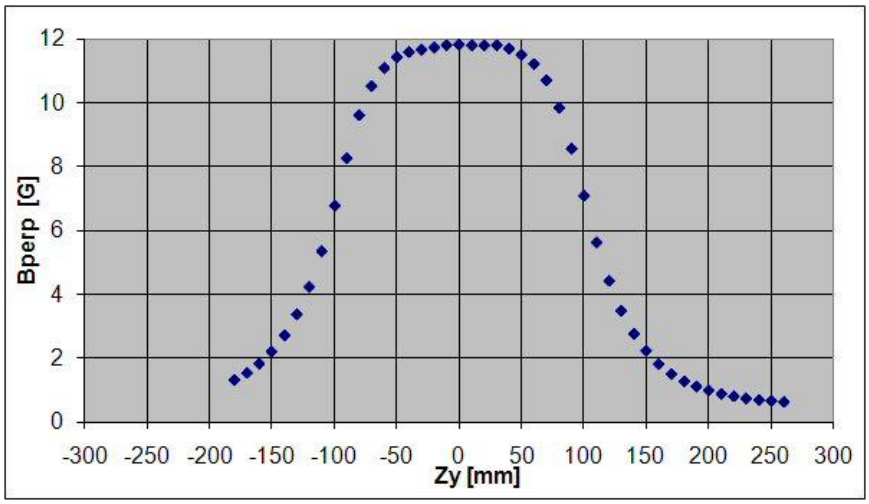

Fig. 15. VD remnant field after ramp up to 50 A and down to 0 A. The field far from the center may also have contributions from ambient (Earth) field, which were not separately measured.

The fringe field beyond the VD dipole ends was mapped using a stair-step current profile, with steps up to 25 A and down to 0 A again. According to Fig. 1, the coils end approximately 120 mm from the center. Data were taken above the lead end (LE) at Z_{Yprobe} = 170 and 260 mm, and below the return end (RE) at Z_{Yprobe} = 210 mm. Figures 16 and 17 show the measurement results (and the individual X,Y probe positions), which indicate a small amount of hysteresis exists (and are consistent with Fig. 14). That there is greater fringe field measured at the LE may be the result of additional contributions from the unshielded magnet power leads in that region. There is also clearly a small axial field component at the ends. The field at 0 A represents the superconductor magnetization contribution plus that of ambient (Earth) field.

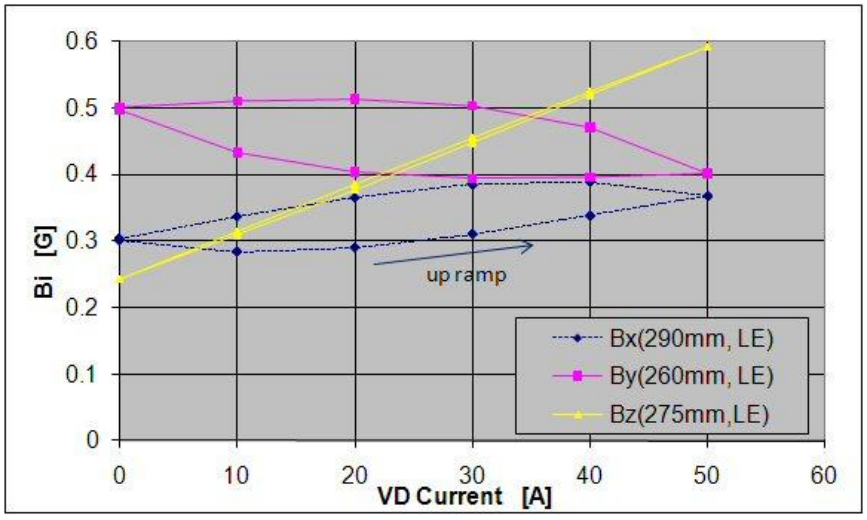

Fig. 16. VD lead end fringe field at Z_{Yprobe} = 260 mm above the dipole center.

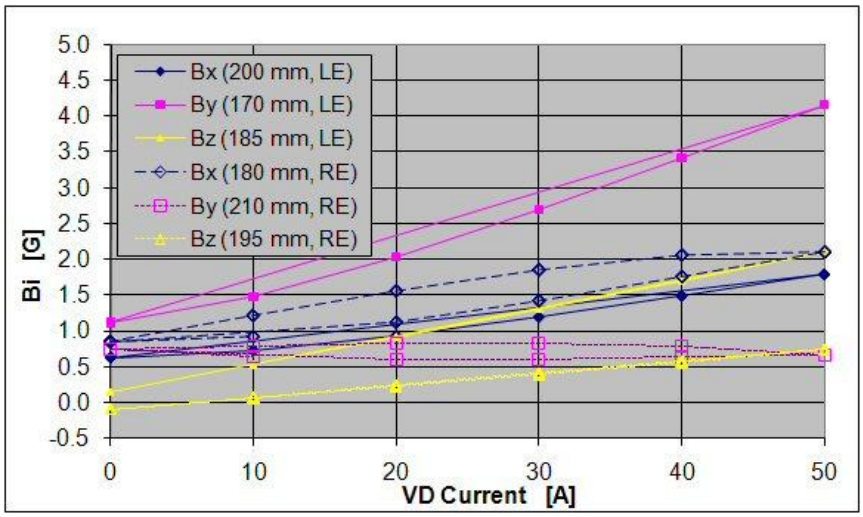

Fig. 17. VD lead end fringe field at Z_{Yprobe} = 170 mm above the dipole center, and return end at Z_{Yprobe} = 210 mm below the dipole center.

VII. Conclusions

The first prototype dipole corrector package for the NML Cryomodule #2 has been fabricated and tested. Both dipoles easily achieved the maximum required integral field strength of 0.01 T-m below the specified 50 A limit: the Outer dipole achieves this field integral at 27.6 A, and the Inner dipole at 28.5 A. Both dipoles in the package reached 100 A current with no spontaneous quenches, and no degradation of performance following a 280 K thermal cycle. The magnetic field strength is very linear up to 100 A current in both dipoles simultaneously.

Fringe fields at both ends of the package were measured at several positions, for the Outer dipole, and are at the level of a few Gauss 250 mm from the magnet center. Also the superconductor plus iron magnetization was measured to be about 2% of the maximum desired field integral – thus it may not be negligible at low current. The superconductor magnetization could be reduced or eliminated by using the heater to quench the coils to a normal resistive state.

Quenches initiated by spot heaters were used to study quench development in one Outer dipole coil. At low current, the quench development is very slow, and the result was similar to what was independently learned in a HINS superconductor strand quench study [4]: the superconductor appears to be sufficiently stabilized that the coils (and leads) are safe. That is to say, if the quench does not propagate to the point where enough voltage develops for detection, the strand is not damaged.

The performance of a strip heater for quench protection of both coils was also studied. Time delay from heater firing until quench detection was measured for a range of coil currents and heater voltages, at the minimum heater power supply capacitance (for shortest pulse length). The trends in quench delay versus heater energy deposition were similar, though the quench development is systematically slower in the Outer coil. The minimum delay, at high current or high heater energy, was comparable to the heater system RC time constant of 25-30 ms. The heaters are not necessary for quench protection if a dump switch and resistor are used; in this case the current decay time constant can be very short. Heaters can provide a redundant protection mechanism. However, similar coils made for the HINS solenoid correctors with smaller diameter (0.3 mm) strand are self-protecting, up to the level of 150 A, without using a

dump resistor [3]. A self-protection test of the CM2 dipoles was not made, however, as a conservative measure to ensure that a working device is available to install in the cryomodule.

This design of a Dipole Corrector, as fabricated and tested, met the required magnetic field properties and exhibited robust performance with large operating margin when working in a bath cooling mode. This result opens the possibility of using this magnet in a conduction cooling mode, and eliminating the LHe vessel, which would simplify magnet installation and adjustment.

VIII. References

1. "TESLA Test Facility Conceptual Design Report", DESY, Germany, http://tesla.desy.de/new_pages/TTFcdrTab.html.
2. G. Davis, et al., "HINS Linac SS-1 Section Prototype Focusing Solenoid Design", TD-08-010, FNAL, March 2008.
3. G. Chlachidze, et al., "HINS_SS1_SOL_02d Fabrication Summary and Test Results," FNAL TD note TD-09-001, January 2009.
4. C. Hess, et al., "HINS_SS1_Sol_03d: Pre-Production SS1 Focusing Lens Fabrication and Test Results,", FNAL TD note TD-10-002, January 2010.
5. D. F. Orris, M. A. Tartaglia, "Superconducting Strand Quench Development Tests," FNAL TD note TD-09-012, May 2009.

IX. Appendix I. Corrector Package for Fermilab CM#2

Corrector Package for Fermilab CM#2

Sergei Nagaitsev

November 19, 2007

Deliverables

Deliverables in this corrector package are (all internal to cryomodule): (1) the superconductive corrector magnets in a cryovessel, (2) the current leads, (3) the instrumentation needed for temperature monitoring and quench protection, (4) interface flanges with feed-throughs. Desired delivery date: Sep 1, 2008.

Layout

The proposed corrector magnet package layout is shown in Fig. 1

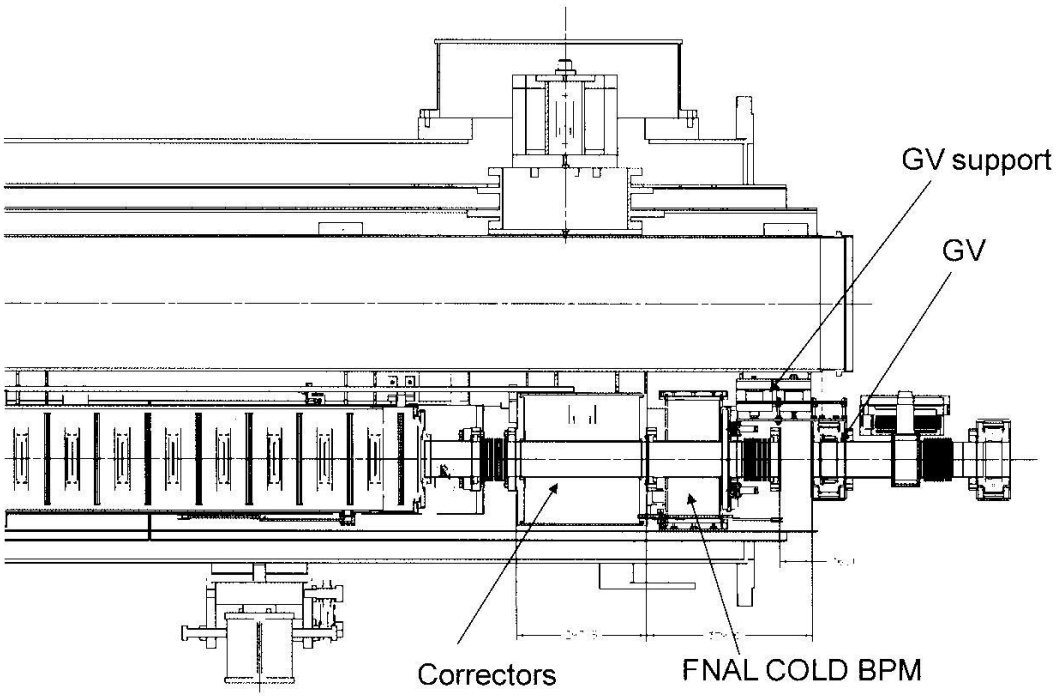

Figure 1: A draft sketch of the corrector package layout in a Type 3+ cryomodule. Corrector magnets are installed in a helium vessel similar to the one designed for the DESY XFEL quad.

The corrector package consists of the following components:

1. Two pairs of superconducting dipole coils operating at 2K LHe. They provide horizontal and vertical correction dipole fields of 0.01 T-m (integral max strength) each. The corrector good-field area diameter is 10 mm with the integrated magnetic field homogeneity of 5%. The corrector package should be effectively shielded to reduce the fringing field in the SCRF cavity

area (20 cm from the corrector cryovessel on axis) to 1 μT during cooling down and 10 μT during operation. Corrector package shall be quench protected. For this reason, voltage taps shall be installed on each corrector coil for quench detection.

2. A helium vessel with an integral beam pipe. The beam pipe shall be SS316L and have the ID of 76.2 mm (3"). It shall be electro-polished and cleaned to UHV specifications. The helium vessel shall be similar in design and overall length to the DESY XFEL Quad vessel. The vessel will be supported from the 300-mm helium pipe using existing brackets (designed for DESY XFEL quad). The vessel beam pipe flanges shall be connected to cavity bellows on one side and to the FNAL cold BPM on the other. The corrector package cold mass length and diameter should be less than 260 mm.

3. Four current leads powering the corrector coils.

Power supply

The dipole correction coils are powered by 4 current lead capable of carrying 100A. We are proposing to use Main Injector Corrector power supplies to power these dipole correctors. These are bi-polar +/- 65A supplies with a quench detection/protection capability. The operating range for correction coils will be +/- 50A .

Thermal loads

The heat load at 2K from the correction coil package shall not exceed 0.1 W.

The heat load at 4K shall not exceed 3W.

Summary

Correction dipoles:

Qty: 2 (horizontal and vertical)

Integral strength: 0.01 T-m (at 50A), this corresponds to 6 mrad angle for a 500-MeV beam

Operating temperature: 2K

Appendix II. Dipole Corrector for NML Cryomodule CM#2

V.S. Kashikhin, October 27, 2008

The dipole corrector specification:

Number of dipole windings	2 (vertical and horizontal)
Integrated strength	0.01 T-m
Peak current	50 A
Operating temperature	2 K
Superconductor	NbTi
Superconductor diameter	0.51 mm (enamel insulated)
Good field area diameter	10 mm
Integrated field homogeneity	5 %
Outer ferromagnetic shield	AISI 1006 – 1010
Cold mass length	260 mm or less

The corrector magnetic field was modeled by TOSCA Opera 3D. The results of field calculations are shown in Fig. 1 – Fig. 4. The peak field in the iron yoke when powered only the vertical dipole coil is 0.38 T. So, the total field in the yoke when powered both dipoles will be less than 0.8 T. The integrated dipole field is 0.02 T-m with the peak field in the magnet center 0.1 T.

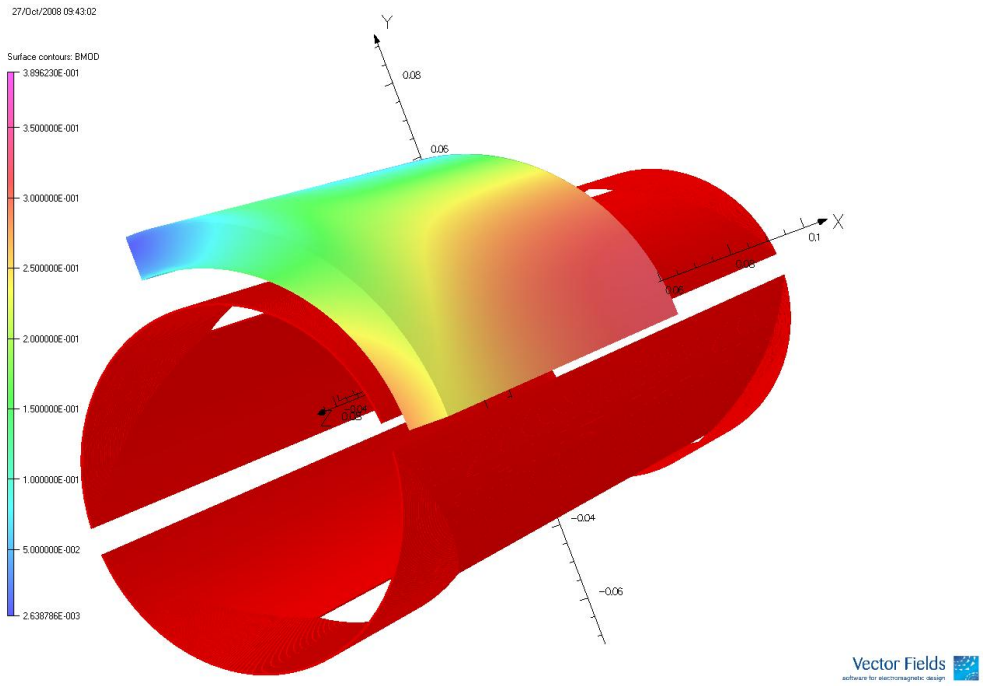

Fig. 1. Dipole corrector 3D model geometry and flux density in the ferromagnetic shield at current 50 A (DCorrector_102308a).

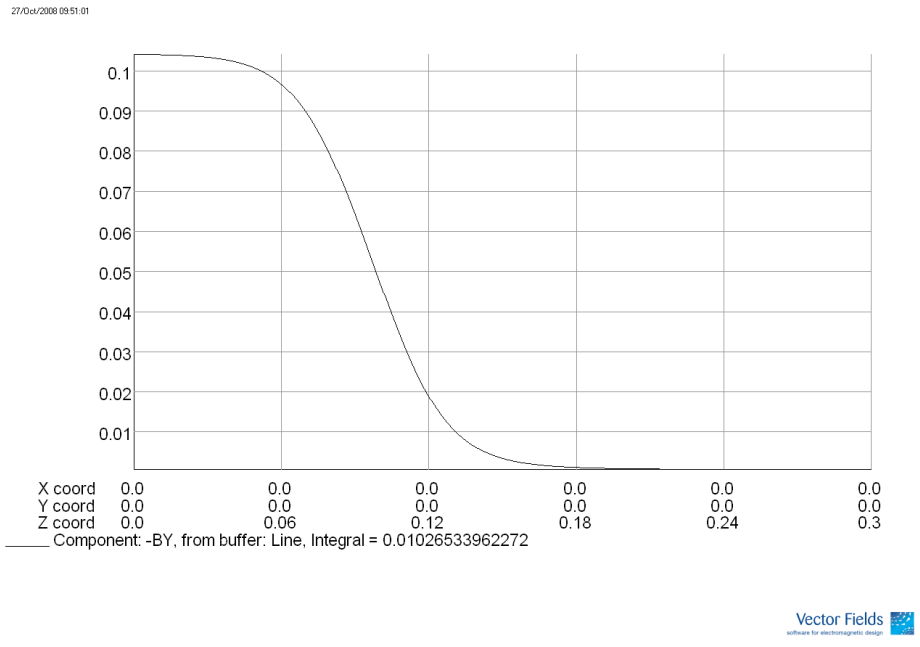

Fig. 2. Field distribution at I=50 A for magnet central longitudinal axis, x=y=0, z=0 - 0.3 m.

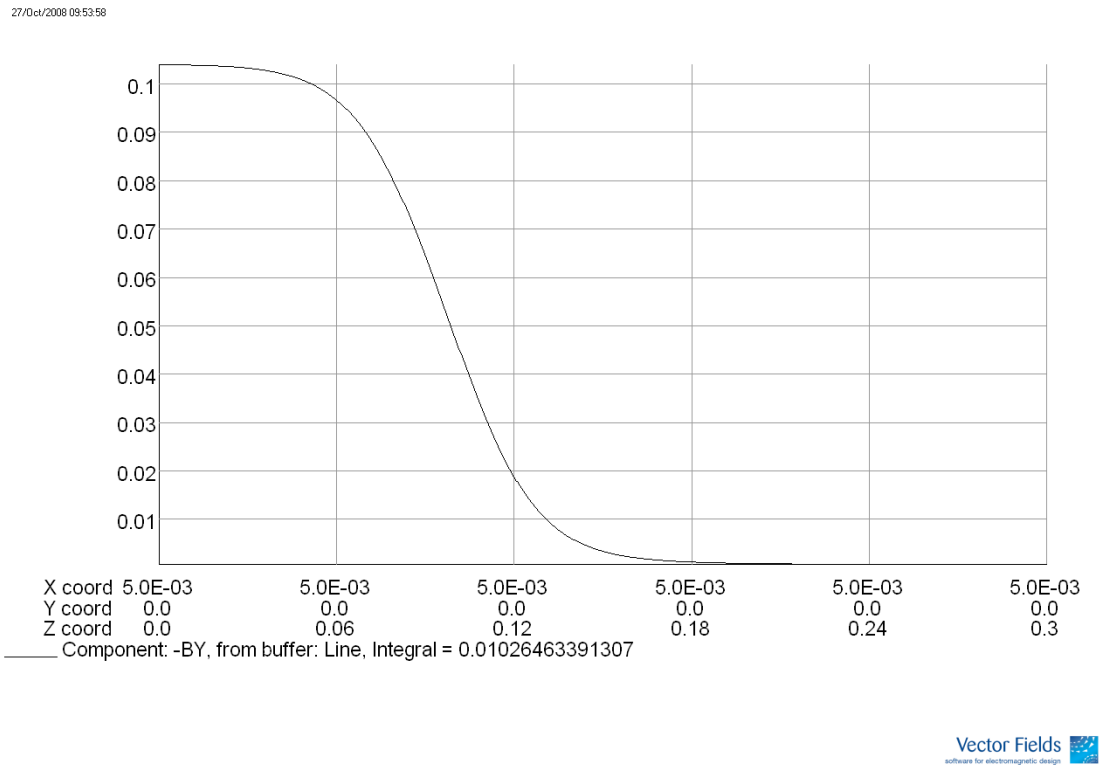

Fig. 3. Field distribution at I=50 A for magnet longitudinal axis, x=5 mm, y=0, z=0 - 0.3 m.

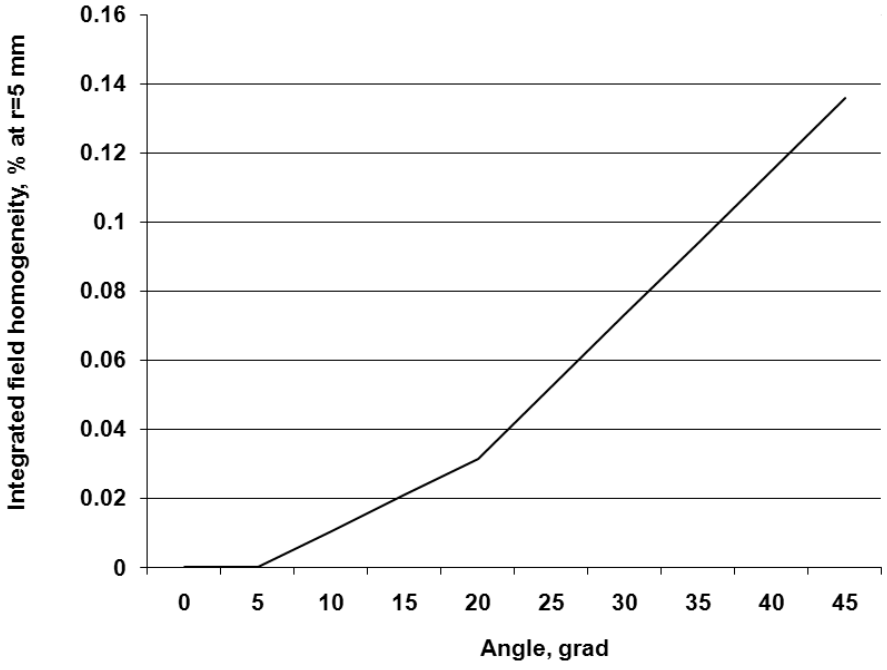

Fig. 4. Vertical Dipole integrated field homogeneity at radius 5 mm.

So, the integrated field homogeneity in the 10 mm diameter area is better than 0.14 % (See Fig. 4).

The proposed for the mechanical design magnet geometry is shown in Fig. 5.

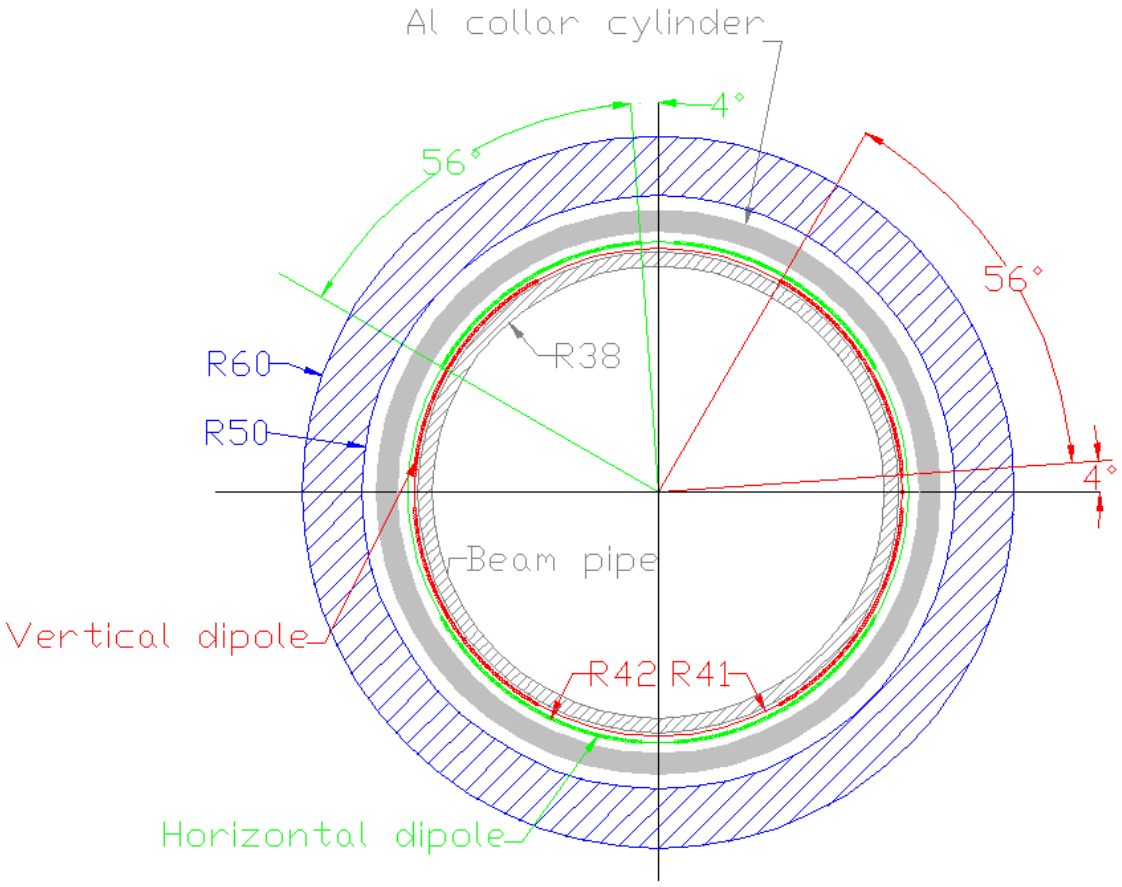

Fig. 5. Dipole corrector cross-section.

The magnet has two shell type of coils glued to the outer surface of the beam pipe. The Al collar cylinder placed outside provides mechanical prestress during cooling down and coil mechanical rigidity. The low carbon steel removable yoke mounted outside the coil assembly and provides proper fringe field shielding. Large current operational margin allows to use corrector without yoke inside future quadrupole doublets.

Dipole corrector design parameters:

Integrated dipole field at 50 A, and 79 turns/pole	0.02 T-m
Integrated field homogeneity in the 10 mm diameter area	0.15 %
Coil length	230 mm
Iron shield length	240 mm